Proflavine and zinc chloride “team chemistry”: combining antibacterial agentsviasolid-state interaction

CrystEngComm

Accepted Manuscript

This article can be cited before page numbers have been issued, to do this please use: C. Fiore, O. Shemchuk, F. Grepioni, R. J. Turner and D. Braga, *CrystEngComm*, 2021, DOI: 10.1039/D1CE00612F.

ROYAL SOCIETY OF CHEMISTRY

rsc.li/crystengcomm

View Article Online
DOI: 10.1039/D1CE00612F

ARTICLE

Proflavine and zinc chloride "team chemistry": Combining antibacterial agents via solid-state interaction.

Cecilia Fiore,[a] Oleksii Shemchuk,[a] Fabrizia Grepioni,[a] Raymond J. Turner*[,b] and Dario Braga*[,a]

Received 00th January 20xx,
Accepted 00th January 20xx

DOI: 10.1039/x0xx00000x

Co-crystallization of the antibacterial agent proflavine (PF) with the inorganic salt $ZnCl_2$ by mechanochemical and solution methods results in the formation of the novel compounds $ZnCl_3$(HPF) (**1**) and $[HPF]_2[ZnCl_4]\cdot H_2O$ (**2**), both containing the proflavinium cation $(HPF)^+$. Both compounds show a 50-125% enhanced antimicrobial activity with respect to the reference standard of $AgNO_3$ and a 25-50% enhancement to the behaviour of the separate components against pathogen indicator strains of *Pseudomonas aeruginosa, Staphylococcus aureus,* and *Escherichia co*li. In terms of crystal structure both compounds $ZnCl_3$(HPF) and $[HPF]_2[ZnCl_4]\cdot H_2O$ are characterized by extensive π-stacking interactions between the proflavine moieties. The same interaction is predominant in the previously unknown crystal structures of neutral proflavine (PF), as well as in that of its dihydrated monochloride salt, $[HPF]Cl\cdot 2H_2O$, which are also described in this paper.

Introduction

Antimicrobial resistance (AMR)[1] is rapidly developing as the major health problems of our time, mainly caused by the abuse of antibiotics to control infections in humans and animals.[2] Most of the common pathogenic strains already have antibiotic-resistant genes and, presumably, more antibiotic-resistant pathogens will emerge in the future.[3] The quest for new antimicrobial agents can nowadays rely on the important conceptual tools provided by crystal engineering[4] namely the possibility of associating within the same crystalline material two or more components[5] via co-crystallization. As a matter of fact, co-crystallization is being actively explored in the pharmaceutical field,[6] since the association of an active ingredient and a coformer, which, in turn, can also be an active molecule, can generate new pharmaceuticals or alter significantly the physico-chemical and pharmokinetic properties of known ones.[7] In the quest for a crystal engineering based answer to the AMR problem, we have recently shown that co-crystallization of the antibacterial compounds proflavine[8] and methyl viologen,[9] with metal salts, such as CuCl, $CuCl_2$ and $AgNO_3$ is a viable, eco-friendly, and inexpensive way to obtain new materials with enhanced antibacterial properties.[10] Analogous co-crystallization approach has been used to prepare new antibacterial active associations of known antibiotics, such as ciprofloxacin, with natural antimicrobials, such as thymol and carvacrol.[11] Based on the same approach a multicomponent solid consisting of an antibacterial (norfloxacin) and an antimicrobial (sulfathiazole) have been recently reported by Desiraju et al.[12] showing enhancement of in vitro biological properties and improved physicochemical behaviour. Beyond organic antimicrobial molecules, metal-based antimicrobials are of great interest as new means of dealing with the AMR threat.[13,14] Silver, zinc, copper and others have been used for millennia as antimicrobial agents.[15] However, the combination of metals with organic antimicrobials as metal-coordinated ligands and/or in co-crystals may represent an alternative resource in the quest for new and diverse solutions.[16] In this work we apply a crystal engineering approach to the preparation, characterization and antimicrobial activity evaluation of two novel compounds obtained from the known antibacterial agent proflavine (see Scheme **1** for neutral proflavine, PF) which is reacted as its hydrochloride proflavinium cation (HPF)+ with zinc chloride. Depending on the stoichiometric ratio between (PFH)+ and zinc chloride and on the preparative conditions the new compounds $ZnCl_3$(HPF) **(1)** and $[HPF]_2[ZnCl_4]\cdot H2O$ **(2)** have been obtained by both solution and mechanochemical methods and characterized by X-ray diffraction, DSC and TGA.

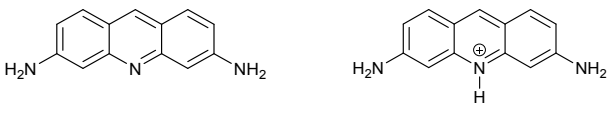

Proflavine (PF) Proflavinium cation (HPF)

Scheme 1. Neutral PF and monoprotonated proflavine HPF used in this work.

The structure of **1** has been determined from powder diffraction data, as it proved impossible to grow single crystals, while that of **2** has been determined from single-crystal X-ray data. Correspondence between the bulk mechanochemical products and the structures of **1** and **2** has been verified by comparing observed and calculated X-ray powder diffraction

[a] *Dipartimento di Chimica "Giacomo Ciamician", Università di Bologna, Via Selmi, 2 – 40126 Bologna – Italy.*
[b] *Department of Biological Sciences, University of Calgary, 2500 University Drive NW, Calgary, Alberta T2N 1N4,*
Electronic Supplementary Information (ESI) available: single crystal and powder X-ray diffraction data, TGA and DSC. See DOI: 10.1039/x0xx00000x

patterns. The mono-hydrate nature of 2 has been ascertained by TGA. The antimicrobial activity of **1** and **2** has been tested against the pathogen indicator strains Pseudomonas aeruginosa ATCC27853, Staphylococcus aureus ATCC25923, and Escherichia coli ATCC 25922. To evaluate the efficacy of the antimicrobials, we have used the established method of measuring a zone of growth inhibition and contact killing using compound impregnated antimicrobial susceptibility filter disk.

In this paper we also report the structural characterization of two novel forms of proflavine, namely the anhydrous proflavine (PF), obtained by dehydration of proflavine monohydrate PF·H_2O (CSD refcode PROFLV[17]), and that of its hydrochloride salt, [HPF]Cl·$2H_2O$, the monoprotonated form of the known dichloride salt [H_2PF]Cl_2·$2H_2O$ (CSD refcode PROFLC[18]). Despite the different nature of the four compounds, the neutral organic molecule (PF), a hydrated salt [HPF]Cl·$2H_2O$, a coordination compound between PF and zinc-chloride **1** and a salt **2**, all these crystals share the common feature of extensive π-stacking and of herring-bone interactions between the proflavine/proflavinium moieties.

Experimental

Materials and methods

All reagents and solvents used in this work were purchased from Sigma-Aldrich and used without further purification.

Preparation of PF·H_2O. Commercial [HPF]$_2$[SO_4]·xH_2O (1 g) was dissolved in 25 mL of water and 3.10 g (0.077 mol) of NaOH was added to the solution, yielding PF·H_2O as a crystalline powder, which was filtered and washed several times with water. The experimental X-ray powder pattern of the product matched the one calculated on the basis of single crystal data for PROFLV (fig. SI-1). A sample of polycrystalline PF·H_2O was analyzed via Hot Stage Microscopy (HSM), using a Linkam TMS94 device connected to a Linkam LTS350 platinum plate and an Olympus optical microscope; heating rate of 10 °C·min^{-1} was applied. Crystal growth of anhydrous proflavine was observed on the original powder at ca. 100 °C, concomitantly with the dehydration process of PF·H_2O. The sample was cooled down to room temperature and the yellow single crystals were structurally characterized analyzed via X-ray diffraction.

Synthesis of PF anhydrous. The anhydrous phase of PF was obtained by thermal treatment in oven for 20 min at 85 °C. The product was characterized by X-ray powder diffraction and the pattern compared with the one calculated from single crystals of PF anhydrous. Single crystals of anhydrous proflavine were obtained directly upon dehydration of PF·H_2O under the microscope during hot-stage heating to 100 °C.

Solution synthesis of $ZnCl_3$(HPF) (1) (PF·H_2O: $ZnCl_2$ = 1:1). A solution of PF·H_2O (113.62 mg, 0.5 mmol) in HCl 0.1 M (2.5 mL, 0.25 mmol) was added to a solution of $ZnCl_2$ (68.14 mg, 0.5 mmol) in water (1 mL). A crystalline powder was recovered after slow evaporation of the solvent and used for structural characterization.

Solution synthesis of [HPF]$_2$[$ZnCl_4$]·H_2O (2) (PF·H_2O : $ZnCl_2$ = 2:1). A solution of PF·H_2O (113.62 mg, 0.5 mmol) in HCl 0.1 M (5 mL, 0.5 mmol) was added to a solution of $ZnCl_2$ (34.07 mg, 0.25 mmol) in water (0.5 mL). A crystalline powder was recovered after slow evaporation of the solvent. Single crystals of **2** were recovered and used for diffraction experiments (see below). Serendipitously, single crystals of [HPF]Cl·$2H_2O$ were also recovered from one of the crystallization batches and submitted to X-ray diffraction.

Solid-state synthesis of $ZnCl_3$(HPF) (1). Crystalline **1** was also obtained by kneading 1:1 stoichiometric amount of [HPF]Cl (obtained by reacting proflavine free base with HCl 0.1M and drying in rotavapor - purity of the product was checked by solution NMR) and $ZnCl_2$, in the presence of 2-3 drops of acetone, for 1 hour in a Retsch MM200 Mixer Mill, operated at a frequency of 15 Hz, with 5 mL agate jars and 2 balls of 5 mm diameter. The same reaction in 2:1 stoichiometric ratio still yielded compound **1**.

Powder X-ray diffraction. For phase identification purposes, room temperature X-ray powder diffraction (XRPD) patterns were collected on a PANalytical X'Pert PRO automated diffractometer equipped with an X'celerator detector in the 2θ range 3–40° (step size 0.011, time/step 50 s, VxA 40x40).

For structural characterization of $ZnCl_3$(HPF) (**1**) from powder data, a room temperature X-ray diffraction pattern was collected in transmission geometry on a PANalytical X'Pert PRO automated diffractometer, equipped with Focusing mirror and Pixcel detector, in the 2θ range 3–60° (step size 0.0130°, time/step 118.32 s, VxA 40kV x 40mA). To improve the quality of the obtained XRPD patterns 3 repetitions were performed and the scans were merged. The compound was indexed in the triclinic P-1 space group with the auto-indexing module of N-TREOR[19] as implemented in the EXPO2014.[20] Simulated annealing method was performed with EXPO2014, using one zinc, three chloride ions and one proflavine cation per asymmetric unit. Ten runs for simulated annealing trial were set, and a cooling rate (defined as the ratio T_n/T_{n-1}) of 0.95 was used. A Rietveld refinement (Fig. ESI-6) was subsequently performed with TOPAS 5.0,[21] treating the proflavine molecule as a rigid body. Structural details are listed in table SI-1.

Single crystal X-ray diffraction. Single Crystal data for **2** as well as for PF and for [HPF]Cl·$2H_2O$ were collected at room temperature with an Oxford Diffraction X´Calibur equipped with a graphite monochromator and a CCD detector. Mo-Kα radiation (λ = 0.71073 Å) was used. Unit cell parameters for both complexes discussed herein are reported in Table S-1. The structure was solved by the Intrinsic Phasing methods and refined by least squares methods against F^2 using SHELXT-2016[22] and SHELXL-2018[23] with Olex2 interface.[24] Non-hydrogen atoms were refined anisotropically. H_{CH} atoms were added in calculated positions; H_{OH} and H_{NH} atoms were either located from a Fourier map or added in calculated positions and refined riding on their respective carbon, nitrogen or oxygen atoms. The software Mercury 4.3[25] was used for graphical representations and for powder patterns simulation on the basis of single crystal data. Crystal data can be obtained free of charge from the Cambridge Crystallographic Data Centre via

View Article Online
DOI: 10.1039/D1CE00612F

https://www.ccdc.cam.ac.uk and have been allocated the accession numbers CCDC 2081498-2081501.

Differential Scanning Calorimetry (DSC). DSC measurements were performed for PF·H_2O, $ZnCl_3$(HPF) **(1)** and $[HPF]_2[ZnCl_4]\cdot H_2O$ **(2)** with a Perkin–Elmer Diamond. The samples (3–5 mg) were placed in sealed aluminium pans, and heating was carried out at 5 °C min^{-1} .

Thermogravimetric analysis (TGA). TGA measurements for PF·H_2O, $ZnCl_3$(HPF) **(1)** and $[HPF]_2[ZnCl_4]\cdot H_2O$ **(2)** were performed using a Perkin-Elmer TGA7 in the temperature range 25-450 °C under an N_2 gas flow, at a heating rate of 5 °C min^{-1}.

Antimicrobial Activity. Antimicrobial efficacy was assessed similarly to previous work[10]. Inoculation from frozen stocks of each of the three bacterium species strains were cultured in test tubes prepared with 2 mL of Luria-Bertani (LB) and incubated at 37°C for 16hrs. These cultures were then used to inoculate spread plates (for zone of inhibition and contact killing). LB agar plates were spread inoculated with 100 µL of overnight culture and were then allowed to dry while disks were prepared. Antimicrobial filter disks (Oxoid Basingstoke Hants, UK Lot# 1872714) were inserted into metal salt or crystal solutions/slurries of 25mg/mL using sterile tweezers to soak and adsorb materials. Disks were exposed for 1-hour with inversions every 15-min. Disks were then placed on the spread plates, all plates received a disk of $AgNO_3$ (also prepared from 25 mg/mL) as the internal control. Plates were incubated overnight at 37°C prior to photography and measuring the zone of inhibition by average diameter (mm). The zones of inhibition were ratioed to the zone of $AgNO_3$ control on each plate to remove plate to plate variances. For contact killing efficacy a pre-grown spread plate received disks to the surface of the bacteria growth lawn and left for 24hrs and then removed to observe clearing of the bacterial growth due to cell lysis (as well as swabbing underneath the disk to see if any exposed bacteria could recover).

Results and Discussion

Proflavine (PF), obtained as a free base from the commercial sulphate salt (see Experimental), was co-crystallized with $ZnCl_2$ both via mechanochemistry (in the form of its chloride salt) and from solution in 1:1 and 2:1 stoichiometric ratios (see Scheme 2), yielding the neutral, anhydrous complex $ZnCl_3$(HPF) (**1**) and the hydrated salt $[HPF]_2[ZnCl_4]\cdot H_2O$ (**2**), both containing the proflavinium cation $(HPF)^+$, i.e. proflavine in its monoprotonated form (see Scheme 1). Crystallization from solution yielded higher purity target products, which were subsequently utilized for the investigation of the antimicrobial activity. It should be stressed here that the term co-crystallization, in this paper as in other related studies,[10] is used to emphasize that the products are obtained via direct mixing of solid compounds that form stable crystalline phases at ambient conditions and that the target of the investigation is the behaviour of the crystalline products in comparison with the crystalline phases of the separate components (*vide infra*).

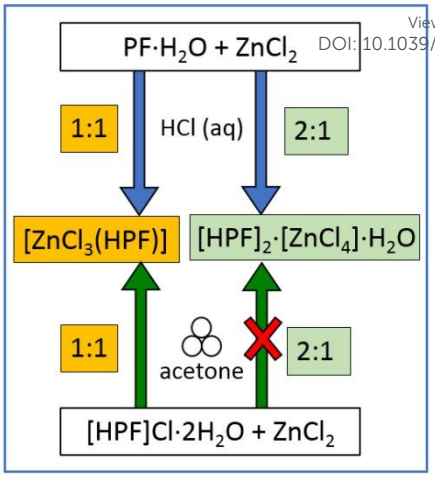

Scheme 2. Different reaction pathways for the synthesis of $ZnCl_3$(HPF) (**1**) and $[HPF]_2[ZnCl_4]\cdot H_2O$ (**2**).

Single crystals of anhydrous proflavine PF were grown directly from polycrystalline PF·H_2O upon dehydration at ca. 100 °C. Figure 1 shows a photograph of the yellow crystals of PF growing from the powder of PF·H_2O while undergoing dehydration under the microscope.

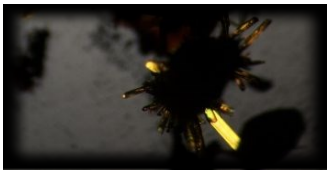

Figure 1. Yellow crystals of anhydrous proflavine, obtained directly upon dehydration of PF·H_2O under the microscope during hot-stage heating to 100°C.

Its structure was determined from single crystal X-ray diffraction data (see ESI) and is characterized by the double herring-bone motif shown in Figure 2, where pairs of PF molecules are stacked along the *b*-axis direction.

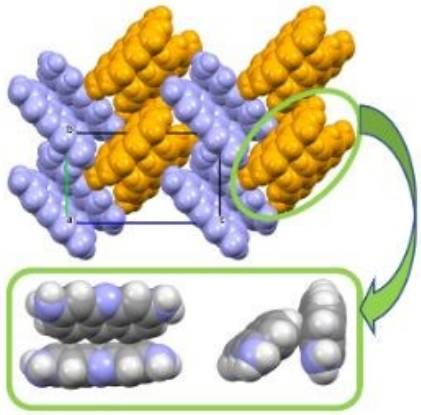

Figure 2. (Top) "double" *herring-bone* pattern in anhydrous PF, and (bottom) front/side views evidencing the C-H···π interactions within a pair of facing molecules.

This arrangement is reminiscent of the one observed in crystalline PF·H_2O (PROFLV), but in this last crystal a simple

herring-bone pattern is present. In both crystals (see inlets in Figures 2 and 3) the PF molecules within a pair are facing each other so as to maximize the number of C-H···π interactions.

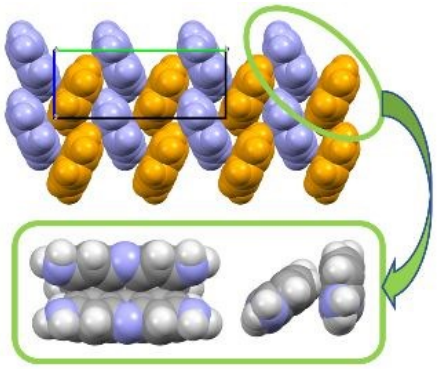

Figure 3. (Top) *Herring-bone* pattern of proflavine molecules in the monohydrated free base PF·H_2O (PROFLV) (water molecules not shown for clarity), and (bottom) front/side views evidencing the C-H···π interactions, analogously to what observed in crystalline PF.

Single crystals of [HPF]Cl·$2H_2O$ were also recovered in one case from the crystallization batch of $[HPF]_2[ZnCl_4]·H_2O$ (**2**) and were subjected to a data collection revealing the unexpected formation of a novel hydrochloride form of PF. It is interesting to note that in this solid, analogously to what observed for the known dichloride salt $[H_2PF]Cl_2·2H_2O$ (PROFLC), the protonation of the acridine nitrogen, and the concomitant presence of good hydrogen bond acceptors – the chloride ion and the water molecule – favor the formation of π-π stacking arrangements of the aromatic units within the crystal, as shown in Figure 4.

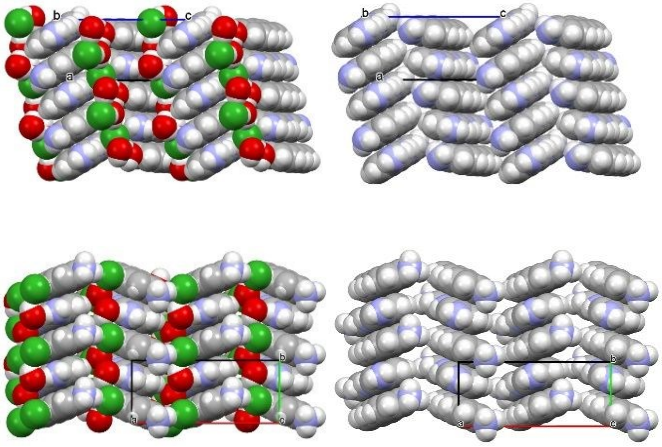

Figure 4. Comparison of the π-stacking arrangements of aromatic mono- and di- cations in the monochloride [HPF]Cl·$2H_2O$ (top) and dichloride $[H_2PF]Cl_2·2H_2O$ (PROFLC) (bottom) proflavine salts. For sake of clarity the cation layers are shown on the right-hand side.

The reaction of proflavine with $ZnCl_2$ in a 1:1 stoichiometric ratio (see experimental) yields the complex $ZnCl_3$(HPF) (**1**), which contains the ligand $(HPF)^+$, i.e. monoprotonated proflavine. Figure 5 shows how $ZnCl_3$(HPF) molecules are piled along the crystallographic *c*-axis, with short interplanar distances of 3.30(1) and 3.37(1) Å.

View Article Online
DOI: 10.1039/D1CE00612F

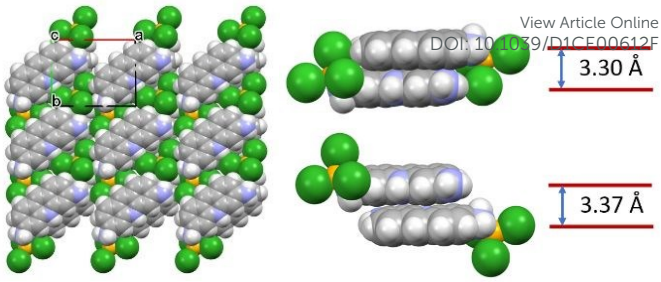

Figure 5. (a) Projection in the *ab*-plane of crystalline $ZnCl_3$(HPF) (**1**). The molecules are arranged in piles along the *c*-axis direction, with short interplanar distances among the aromatic moieties (b).

Reaction of proflavine with $ZnCl_2$ in a 2:1 stoichiometric ratio (see experimental) yields the hydrated molecular salt $[HPF]_2ZnCl_4·H_2O$ (**2**), which contains monoprotonated proflavine as a counterion, instead of coordinated ligand as in compound **1**. Figure 6 shows how pairs of proflavinium cations are π-stacked in the crystal, with pairs arranged in a herring-bone fashion; interplanar distances are 3.34(1) and 3.41(1) Å (see fig. 6).

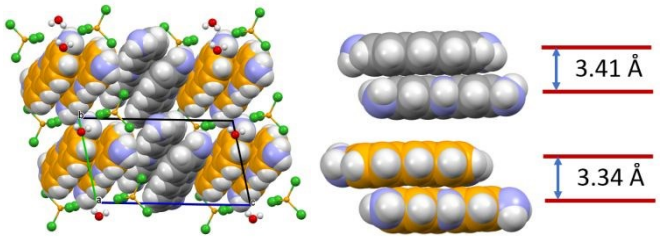

Figure 6. Projection down the crystallographic *b*-axis of crystalline $[HPF]_2[ZnCl_4]·H_2O$ (**2**), showing the herring-bone pattern of HPF^+ cationic pairs (a) and the π-stacking arrangement of the cations within each pair (b; compare with crystalline **1** in Fig. 5). (Grey and orange spheres represent the carbon atoms belonging to the two independent molecules)

A standard antimicrobial disk-diffusion approach[26] was used to evaluate relative antimicrobial activity. Both proflavine and zinc are antimicrobial and the question here is if they would retain their antimicrobial activity in a co-crystal. Rather than reporting absolute zone of inhibition of growth, the amount of inhibition was ratioed for comparison to $AgNO_3$ (Figure 7). Silver is the most established metal-based antimicrobial[27] and thus is an excellent comparator to evaluate new formulations. Under the media conditions used here, $AgNO_3$ gives minimal inhibitory concentration value of 0.125 mM towards all three bacterial strains used here.[28] We see that $ZnCl_2$ has similar efficacy as $AgNO_3$ to *P. aeruginosa,* but slightly better efficacy towards *E. coli* and best for *S. aureus*. Proflavine is a planar molecule that effectively intercalates into DNA as its mode of toxicity, making it an effective antimicrobial antiseptic and potential anticancer agent.[29] Proflavine shows higher antimicrobial activity than silver in our assays. Combining the two compounds shows a 50 to 125% better efficacy than $AgNO_3$ towards all three of the pathogen indicator strains we tested. Additionally, all compounds had contact killing against all three strains. This was evaluated by placing the compound impregnated disks onto a

View Article Online
DOI: 10.1039/D1CE00612F

lawn of live bacteria and assessing the ability to kill the bacterial in contact. This data demonstrates that the mixture as a crystal did not decrease the biocidal activity of the compounds and potentially enhances them, which was unexpected and somewhat remarkable. Given that the crystal mixtures by weight would actually have less proflavine by moles, the data implies the presence of the Zn enhances the antimicrobial efficacy of proflavine more than what one interprets from Figure 7.

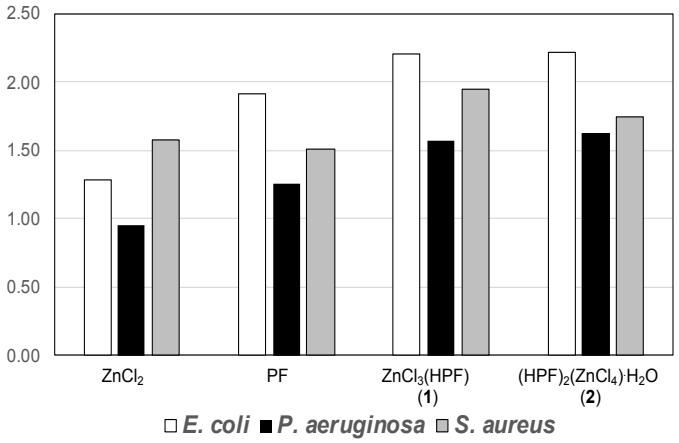

Figure 7. Fold antimicrobial activity compared to $AgNO_3$ (the value of 1.00 is equal efficacy as silver nitrate). Data from 3 independent biological trials (2 technical trials each) are given, variance between trials was removed through ratioing to a control on each plate (silver nitrate) which leads to negligible differences in fold activity.

Conclusions

The increasing concern in the development of antimicrobial resistance is motivating the quest for new materials to be used in the battle against pathogens. A promising approach is that of using co-crystallization to synthesise new materials and/or to enhance the properties of active molecules. With this idea in mind we have prepared by both solution and solid-state methods and structurally characterized two novel compounds of the antibacterial proflavine with $ZnCl_2$, namely $ZnCl_3$(HPF) (**1**) and $[HPF]_2[ZnCl_4]\cdot H_2O$ (**2**). Interestingly, **1** can be obtained mechanochemically as the unique product when starting from $[HPF]Cl\cdot 2H_2O$ while reaction in solution from $PF\cdot H_2O$ and $ZnCl_2$ yields **1** or **2** depending on whether a 1:1 or 2:1 stoichiometric ratio of the reactants is used. The fact that mechanochemical and solution synthesis may yield different products is not surprising[30] and has been observed in several cases. In terms of antimicrobial activity the two compounds appear to be from 1.5 to 2 times more efficient towards the pathogen indicator strains with respect to the reagents and towards $AgNO_3$ used as a standard of metal antimicrobial activity. We envisage the use of our compounds as coating materials in the prevention of infectious disease transfer or microbial fouling. The challenges that exist is producing a crystal that releases the active ingredients at a level that sustains antimicrobial properties and that is stable to the physical manipulation and use of the material that has been coated. This opens avenues for development of unique metal chelates and organo-metal compounds for AMB applications.

Conflicts of interest

There are no conflicts to declare.

Acknowledgements

This material is based upon O.S. D.B., F.G. work supported by the University of Bologna (RFO scheme). NSERC supported the contribution of R.J.T.
R.J.T. thanks Dylan Greening for his assistance. The help of Dr. Lucia Casali (structure solution from X-ray powder data) and Dr. Katia Rubini (DSC/TGA) is gratefully acknowledged. The contribution of Marzia Guerrini as a part of her master thesis under D.B. supervision is acknowledged.

Notes and reference

1 S. B. Levy and M. Bonnie, *Nat. Med.*, 2004, 10, S122–S129
2 E. D. Brown and G. D. Wright, *Nature*, 2016, 529, 336–343.
3 L. M. Streicher, *J. Glob. Antimicrob. Resist.*, 2021, 24, 285–295.
4 G. R. Desiraju, *Angew. Chemie Int. Ed.*, 2007, **46**, 8342–8356.
5 Ö. Almarsson and M. J. Zaworotko, *Chem. Commun.*, 2004, 0, 1889–1896.
6 J. Wouters, L. Quéré, *Pharmaceutical salts and co-crystals*, Royal Society of Chemistry, 2011.
7 N. Schultheiss and A. Newman, *Cryst. Growth Des.*, 2009, 9, 2950–2967.
8 M. Wainwright, *J. Antimicrob. Chemother.*, 2001, **47**, 1–13.
9 M. C. Sulavik, C. Houseweart, C. Cramer, N. Jiwani, N. Murgolo, J. Greene, B. Didomenico, K. J. Shaw, G. H. Miller, R. Hare and G. Shimer, *Antimicrob. Agents Chemother.*, 2001, **45**, 1126–1136.
10 O. Shemchuk, D. Braga, F. Grepioni and R. J. Turner, *RSC Adv.*, 2020, **10**, 2146–2149.
11 O. Shemchuk, S. D'Agostino, C. Fiore, V. Sambri, S. Zannoli, F. Grepioni and D. Braga, *Cryst. Growth Des.*, 2020, **20**, 6796–6803.
12 S. P. Gopi, S. Ganguly and G. R. Desiraju, *Mol. Pharm.*, 2016, **13**, 3590–3594.
13 R. J. Turner, *Microb. Biotechnol.*, 2017, **10**, 1062–1065.
14 J. A. Lemire, J. J. Harrison and R. J. Turner, *Nat. Rev. Microbiol.*, 2013, **11**, 371-384.
15 J. W. Alexander. *History of the medical use of silver. Surg Infect (Larchmt),* 2009, **10**, 289-292.
16 A. S. Abd-El-Aziz, C. Agatemor and N. Etkin, *Biomaterials,* 2017, **118**, 27-50.
17 A. Achari and S. Neidle, *Acta Crystallogr. Sect. B Struct. Crystallogr. Cryst. Chem.*, 1976, **32**, 2537–2539.
18 S. K. Obendorf, H. L. Carrell and J. P. Glusker, *Acta Crystallogr. Sect. B Struct. Crystallogr. Cryst. Chem.*, 1974, **30**, 1408–1411.
19 A. Altomare, C. Giacovazzo, A. Guagliardi, A. G. G. Moliterni, R. Rizzi and P. E. Werner, *J. Appl. Crystallogr.*, 2000, **33**, 1180–1186.
20 A. Altomare, C. Cuocci, C. Giacovazzo, A. Moliterni, R. Rizzi, N. Corriero and A. Falcicchio, *J. Appl. Crystallogr.*, 2013, **46**, 1231–1235.
21 A. A. Coelho, *J. Appl. Crystallogr.*, 2018, **51**, 210–218.
22 G. M. Sheldrick, *Acta Crystallogr. Sect. A Found. Crystallogr.*, 2015, **71**, 3–8.
23 G. M. Sheldrick, *Acta Crystallogr. Sect. C Struct. Chem.*, 2015, **71**, 3–8.

View Article Online
DOI: 10.1039/D1CE00612F

24 O. V. Dolomanov, L. J. Bourhis, R. J. Gildea, J. A. K. Howard and H. Puschmann, *J. Appl. Crystallogr.*, 2009, **42**, 339–341.
25 C. F. MacRae, I. Sovago, S. J. Cottrell, P. T. A. Galek, P. McCabe, E. Pidcock, M. Platings, G. P. Shields, J. S. Stevens, M. Towler and P. A. Wood, *J. Appl. Crystallogr.*, 2020, **53**, 226–235.
26 M. Balouiri, M. Sadiki and S. K. Ibnsouda, *J. Pharm. Anal.*, 2016, 6, 71–79.
27 J. S. Möhler, W. Sim, M. A. T. Blaskovich, M. A. Cooper and Z. M. Ziora, *Biotechnol. Adv.*, 2018, 36, 1391–1411.
28 A. Pormohammad and R. J. Turner, *Antibiotics*, 2020, **9**, 853.
29 V. M. Hridya, J. T. Hynes and A. Mukherjee, *J. Phys. Chem. B*, 2019, **123**, 10904–10914.
30. S. L. James, C. J. Adams, C. Bolm, D, Braga, P. Collier, T, Friščić, F. Grepioni, K. D. M. Harris, G. Hyett, W. Jones, A. Krebs, J. Mack, L. Maini, A. G. Orpen, I. P. Parkin, W. C. Shearouse, J. W. Steed, D. C. Waddell, D. C. *Chem. Soc. Rev.* **2012,** *41*, 413-447.